ReGeo ISSN: 2177-3246

MODELING AND OPTIMIZATION OF REVERSE CATIONIC FLOTATION OF IRON ORE USING NEURAL NETWORKS

MODELAGEM E OTIMIZAÇÃO DA FLOTAÇÃO CATIÔNICA REVERSA DE MINÉRIO DE FERRO COM USO DE REDES NEURAIS

MODELADO Y OPTIMIZACIÓN DE LA FLOTACIÓN CATIÓNICA REVERSA DE MINERAL DE HIERRO MEDIANTE REDES NEURONALES

https://doi.org/10.56238/revgeov17n7-119

Data de submissão: 06/06/2026 **Data de publicação:** 21/07/2026

Helen Marques Martins[1], **Christiano Pedro Guirlanda**[2], **Eduarda de Aquino Santos e Silva**[3], **Klarisse Rodrigues Gomes**[4], **Diego Henrique de Souza**[5], **Juan Canellas Bosch Neto**[6]

ABSTRACT

Geometallurgical variability in the feed of iron ore flotation circuits represents a continuous challenge for operational stability and concentrate quality assurance. The use of traditional collectors can cause excessive froth generation when associated with increasingly complex ores and process waters, creating physical bottlenecks and selectivity losses. In this context, the present study aimed to evaluate the metallurgical performance of a standard collector, FLOTIGAM 7500, compared to a low-foaming collector, FLOTIGAM 8525, in an industrial reverse cationic flotation circuit in the Iron Quadrangle. To map the dynamic behavior of the process during the processing of a homogenization stockpile, computational modeling was carried out using Artificial Neural Networks (ANNs) of the Multilayer Perceptron (MLP) type. After multiscale temporal alignment of the industrial data, the trained models were subjected to parametric sweep simulations to decode the physicochemical signatures of each reagent. The results indicated a window of metallurgical convergence in feed scenarios above 23.5% iron content, where both reagents achieved comparable and satisfactory metallurgical performance. However, under critical conditions of depleted ore, with feed iron contents below 20.0%, performance diverged markedly. The standard collector FLOTIGAM 7500 demonstrated high operational robustness, stabilizing iron losses in the tailings at 4.0%, at the cost of a 7.0% increase in silica in the concentrate. In contrast, the new reagent FLOTIGAM 8525 showed high chemical selectivity, reducing silica in the concentrate to 2.0%; however, its reduced froth generation led to lower selectivity, causing a significant increase in iron losses in the tailings. It is concluded that the technological replacement by FLOTIGAM 8525 is highly promising for increasing product purity, but requires the implementation of advanced dosage control logic during periods of declining feed grade, to mitigate the risk of mass loss.

[1] Master's student in Engenharia Química. Federal University of São João del Rei (UFSJ).
E-mail: helenmmartins@gmail.com Orcid: https://orcid.org/0009-0006-7812-2835
[2] Postdoctoral in Engenharia Química. Federal University of São João del Rei (UFSJ).
E-mail: alimenttos@gmail.com Orcid: https://orcid.org/0000-0002-7909-6951
[3] Engenharia Química student. Federal University of São João del Rei (UFSJ).
E-mail: eduardaaquino07@aluno.ufsj.edu.br
[4] Engenharia Química student. Federal University of São João del Rei (UFSJ).
E-mail: klarisse.gomes2015@aluno.ufsj.edu.br
[5] Engenheiro Químico. Federal University of São João del Rei (UFSJ). E-mail: dizzpvd@gmail.com
[6] Professor do curso de Engenharia Química. Federal University of São João del Rei (UFSJ).
E-mail: jboschbr@ufsj.edu.br Orcid: https://orcid.org/0000-0002-2719-7689

Keywords: Flotation. Iron Ore. Artificial Neural Networks. Collectors. Process Simulation.

RESUMO
A variabilidade geometalúrgica na alimentação de circuitos de flotação de minério de ferro representa um desafio contínuo para a estabilidade operacional e a garantia da qualidade do concentrado. O uso de coletores tradicionais pode causar maior espumação quando associado a minérios e águas de processo cada vez mais complexos, gerando gargalos físicos e perdas de seletividade. Neste contexto, o presente trabalho teve como objetivo avaliar a performance metalúrgica de um coletor padrão FLOTIGAM 7500 em comparação com um coletor de baixa espumação FLOTIGAM 8525 em um circuito industrial de flotação catiônica reversa do Quadrilátero Ferrífero. Para mapear o comportamento dinâmico do processo sob a influência de uma pilha de homogeneização, utilizou-se a modelagem computacional por meio de Redes Neurais Artificiais (RNAs) do tipo Multilayer Perceptron (MLP). Após o alinhamento temporal multiescala dos dados industriais, os modelos treinados foram submetidos a simulações de varredura paramétrica para decodificar as assinaturas físico-químicas de cada reagente. Os resultados indicaram uma janela de convergência metalúrgica em cenários de alimentação acima 23,5% de teor de ferro, onde ambos os reagentes atingiram performances boas e similares. No entanto, sob condições críticas de minério empobrecido, com teores abaixo de 20,0% de ferro na alimentação, os desempenhos divergiram drasticamente. O coletor padrão FLOTIGAM 7500 demonstrou elevada robustez operacional, estabilizando as perdas de ferro no rejeito em 4,0%, ao custo de um aumento de 7,0% de sílica no concentrado. Em contrapartida, o novo reagente FLOTIGAM 8525 apresentou elevada seletividade química, reduzindo a sílica no concentrado para 2,0%; contudo, sua baixa taxa de espumação induziu a uma menor seletividade provocando um aumento significativo de perdas de ferro no rejeito. Conclui-se que a substituição tecnológica pelo FLOTIGAM 8525 é altamente promissora para a elevação da pureza do produto, mas exige a implementação de lógicas de controle avançado da dosagem do coletor durante períodos de queda no teor da alimentação, mitigando os riscos de perda de massa.

Palavras-chave: Flotação. Minério de Ferro. Redes Neurais Artificiais. Coletores. Simulação de Processos.

RESUMEN
La variabilidad geometalúrgica en la alimentación de los circuitos de flotación de mineral de hierro representa un desafío continuo para la estabilidad operacional y la garantía de calidad del concentrado. El uso de colectores tradicionales puede causar mayor espumación cuando se asocia a minerales y aguas de proceso cada vez más complejos, generando cuellos de botella físicos y pérdidas de selectividad. En este contexto, el presente trabajo tuvo como objetivo evaluar el desempeño metalúrgico de un colector estándar FLOTIGAM 7500 en comparación con un colector de baja espumación FLOTIGAM 8525 en un circuito industrial de flotación catiónica reversa del Cuadrilátero Ferrífero. Para mapear el comportamiento dinámico del proceso bajo la influencia de una pila de homogeneización, se utilizó el modelado computacional mediante Redes Neuronales Artificiales (RNA) del tipo Multilayer Perceptron (MLP). Tras el alineamiento temporal multiescala de los datos industriales, los modelos entrenados fueron sometidos a simulaciones de barrido paramétrico para decodificar las firmas fisicoquímicas de cada reactivo. Los resultados indicaron una ventana de convergencia metalúrgica en escenarios de alimentación superiores al 23,5% de tenor de hierro, donde ambos reactivos alcanzaron desempeños buenos y similares. Sin embargo, en condiciones críticas de mineral empobrecido, con tenores inferiores al 20,0% de hierro en la

alimentación, los desempeños divergieron drásticamente. El colector estándar FLOTIGAM 7500 demostró una elevada robustez operacional, estabilizando las pérdidas de hierro en el relave en 4,0%, a costa de un aumento del 7,0% de sílice en el concentrado. En contrapartida, el nuevo reactivo FLOTIGAM 8525 presentó una elevada selectividad química, reduciendo la sílice en el concentrado a 2,0%; sin embargo, su baja tasa de espumación indujo una menor selectividad, provocando un aumento significativo de las pérdidas de hierro en el relave. Se concluye que la sustitución tecnológica por el FLOTIGAM 8525 es altamente prometedora para la elevación de la pureza del producto, pero exige la implementación de lógicas de control avanzado de la dosificación del colector durante los períodos de caída del tenor de la alimentación, mitigando los riesgos de pérdida de masa.

Palabras clave: Flotación. Mineral de Hierro. Redes Neuronales Artificiales. Colectores. Simulación de Procesos.

1 INTRODUCTION

Iron ore mining plays a central role in Brazil's economy and trade balance. With the progressive depletion of high-grade iron ore deposits, which are composed mainly of compact hematite, the mining industry has increasingly relied on itabirites and low-grade ores. This scenario has imposed new technical challenges on beneficiation plants, making the ore concentration step a critical factor for the economic feasibility of projects and for meeting the strict chemical specifications required by the global steel market (Lima *et al*., 2013; Rocha *et al*., 2010).

In this context, reverse cationic flotation has emerged as the main technological route for iron ore concentration in Brazil. The process is based on the depression of iron oxides, typically using gelatinized corn starch, and on the flotation of siliceous gangue through the addition of cationic collectors, predominantly etheramines (Araújo *et al*., 2005; Filippov *et al*., 2014; Peres *et al*., 2007).

Industrial-scale operation faces continuous dynamic disturbances governed by the mineralogical variability of the feed ore and by reagent–equipment interactions and circuit hydrodynamics (Chaves, 2006).

In large-scale plants, the use of conventional commercial etheramines, such as the industrial collector FLOTIGAM 7500, often presents operational challenges associated with circuit stability and the broad geometallurgical variability of the feed ore. Although this reagent exhibits excellent metallurgical selectivity under controlled conditions, ensuring that the iron and silica grades specified for the concentrate are achieved, mineralogical complexity combined with process-water recirculation can lead to excessive and uncontrolled froth generation. This phenomenon is intensified by fluctuations in slimes circuit control, a stage that precedes flotation. In the industrial plant evaluated in this study, located in the Iron Quadrangle and equipped with column flotation technology, the disproportionate froth volume collapses the flow regime in the transfer boxes and induces frequent cavitation events in the slurry pumps, forcing sudden shutdowns for physical unclogging of the system. These events result in reductions in the overall plant feed rate and compromise the hydrodynamic stability of the circuit, which is a fundamental requirement for efficient ore treatment, especially in the concentration stage (Papini *et al*., 2001).

To address this process-related occurrence, Clariant developed an alternative low-foaming collector, FLOTIGAM 8525, specifically designed for ores with higher froth-generation potential.

In the technical literature and in industrial practice, however, there is ongoing controversy regarding the replacement of standard reagents with low-foaming product lines. Several studies indicate that changes in froth structure may reduce froth stability or decrease the collector's hydrophobizing capacity, the flotation kinetics of silica, and, consequently, the collecting power. As a result, there is concern that froth reduction may require higher dosages of the new reagent or lead to undesirable iron losses to the tailings or to a loss of concentrate quality (Wang *et al*., 2015).

Validating efficiency at industrial scale is challenging, since even traditional statistical methods often lack the capacity to isolate the process and mineralogical noise intrinsic to ore beneficiation. In view of this, this study addresses the need to apply a more advanced methodology capable of assessing the actual behavior of the new product under highly variable industrial conditions, testing its technical feasibility without penalizing the overall efficiency of the circuit (Napier-Munn, 2014).

Given the complexity involved in evaluating multivariable industrial tests, the application of computational tools based on simulations and capable of assessing different scenarios represents the frontier of innovation in process engineering. The integration of massive databases collected by online instrumentation systems (PIMS) with laboratory X-ray fluorescence (XRF) analyses enables comprehensive mapping of the plant's operational variables. The scope of this research is limited to the study of this multiscale database, collected during the processing of a homogenization stockpile at the plant (Ali; Frimpong, 2020).

To overcome the limitations of direct comparative analysis and predict the metallurgical behavior of the plant under varying collector conditions, this study proposes the use of machine learning techniques. Specifically, the use of Artificial Neural Networks (ANNs) of the Multilayer Perceptron (MLP) type is particularly notable for its ability to map nonlinear relationships, capture the stochastic dynamics of the process, and generalize operational patterns. By submitting operational data to this computational training, it becomes possible to improve the effectiveness of process analysis, considering all the most relevant complex variables, and to comparatively evaluate the collectors in order to provide the process team with a model that supports technical decision-making regarding the most suitable product, as well as a deeper analysis of flotation efficiency itself (Jorjani *et al*., 2009).

The strategic relevance and innovative nature of this research were supported by a systematic bibliometric mapping conducted in the Scopus and Web of Science databases,

covering the period from 2000 to 2025. The initial investigation revealed a notable scarcity of studies strictly dedicated to the intersection between Artificial Intelligence (AI), artificial neural networks, and reverse iron ore flotation, yielding only four articles common to both indexing platforms when the most restrictive keyword combination was applied. These findings confirm the historically conservative stance of the mining industry in incorporating disruptive computational technologies, with most publications on artificial intelligence appearing only in recent years (post-2020). Thus, the development of a model using artificial neural networks was conducted with real historical data from an industrial plant.

The objective of this study was to develop and validate a model using Multilayer Perceptron (MLP) Artificial Neural Networks and to compare, at industrial scale, the performance of two cationic collectors in flotation—the standard reagent FLOTIGAM 7500 and the low-foaming reagent FLOTIGAM 8525—in an iron ore circuit.

To achieve the proposed general objective, the following specific objectives were defined: to integrate and process multiscale operational data; to harmonize semicontinuous online instrumentation data (PIMS) with discrete laboratory chemical analyses (XRF), applying data cleaning and quadratic imputation techniques to correct signal failures in dosage variables; to evaluate performance through modeling for stockpile 1, verifying the network's capability in relation to stockyard mineralogical variability and reagent transition; to calibrate the model's generalization capacity; to optimize the ANN parameters and the Levenberg-Marquardt training algorithm to achieve a rigorous correlation coefficient (R) of at least 0.85, ensuring adherence to industrial data without overfitting; and to compare the efficiency of the tested collectors using simulation responses and operational data analysis in order to verify whether the low-foaming collector (FLOTIGAM 8525) delivers metallurgical performance equivalent or superior to that of the standard collector, thereby justifying or not its adoption to minimize handling and operational issues in the circuit.

2 THEORETICAL FRAMEWORK

Flotation is a concentration process that separates solid particles by exploiting differences in surface characteristics among the various mineral species present. For ore concentration by flotation to be successful, three basic requirements must be met: liberation of the minerals of interest, differentiation of the properties or characteristics of the minerals to be separated, and dynamic separability (Valadão; Araújo, 2012).

Starch gelatinized with caustic soda is one of the universal depressants for iron oxides in iron ore flotation. Starch preferentially interacts with iron oxides, modifying their surface and rendering them hydrophilic (Chaves, 2009).

In reverse iron ore flotation, a pH range between 9 and 10.5 is used, as shown in Figure 1: quartz exhibits higher amine-driven floatability within this pH range, since the quartz to be floated has a negative zeta potential at this pH range and is collected by the positively charged polar group of the amine (Lima; Quirino, 2003).

Figure 1

Quartz floatability percentage as a function of pH and different etheramine concentrations

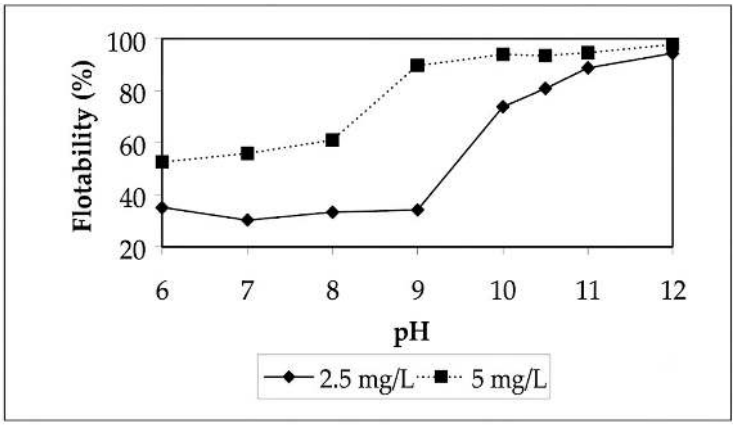

Source: Lima & Quirino (2003).

The FLOTIGAM™ 7500 and FLOTIGAM™ 8525 collector products, supplied by Clariant, are commercial flotation collectors used for the removal of quartz and other silicate minerals from iron ore. Through their chemical formulation, more selective adsorption is achieved on the surface of these gangue minerals, providing improved flotation performance in terms of iron recovery and concentrate grades. The term deep learning refers to a field of machine learning that involves neural networks with multiple layers. These networks are designed to learn increasingly complex and abstract data representations through successive processing layers. The objective is to enable artificial intelligence (AI) systems to perform tasks more efficiently than traditional methods, such as image processing, speech recognition, and data analysis (Pouyanfar *et al*., 2018).

3 METHODOLOGY

This research originated from a real operational optimization demand at an iron ore beneficiation plant located in the Iron Quadrangle, in Minas Gerais, Brazil. The reverse

cationic flotation circuit at the unit has historically operated using the FLOTIGAM 7500 collector, a standard commercial etheramine. Although the standard reagent delivers the selectivity and grades specified for the final concentrate, mineralogical and granulometric changes in the ore have caused severe operational disturbances due to excessive froth generation in the flotation circuit and in the slurry transfer boxes, resulting in operational shutdowns, ore losses, and productivity losses, compounded by a high rate of process-water recirculation in the flotation circuit.

Uncontrolled froth generation collapsed the hydrodynamic regime of the pumps, frequently inducing cavitation, with product losses in the transfer boxes and widespread overflow conditions. As a direct consequence, the operating team was forced to stop plant production for circuit cleaning and stabilization, leading to losses in the overall production rate of the plant.

To mitigate this logistical and production bottleneck, inherent to the mineral characteristics of specific ore fronts in the mine and to the high recirculation of process water, an industrial trial of the FLOTIGAM 8525 collector was designed and conducted. This new reagent has a chemical composition designed to act as a low-foaming collector, with the expectation of delivering metallurgical performance similar to that of FLOTIGAM 7500 in terms of concentrate grade, while eliminating episodes of excessive frothing and unplanned plant shutdowns.

The mineralogical fluctuations of the run-of-mine ore (ROM) represent the primary source of process noise capable of masking the results of comparative industrial tests. To isolate this disturbance variable and ensure that both collectors were tested under an identical mineral matrix, a strategy based on monitoring a single ore homogenization stockpile, stockpile 1, was adopted. The plant relies on a stockyard system in which homogenization stockpiles are formed sequentially, with plant consumption times ranging from four to six days of continuous feed.

For this experiment, focused on the qualification stage, stockpile 1 was divided into two equal halves based on its total accumulated volume: one half was processed using the standard collector, FLOTIGAM 7500, and the other half using the low-foaming collector, FLOTIGAM 8525. This division ensured stable operational windows of two to three days for each product under the same geological profile and under the same intrinsic mineralogical constraints of the mine.

The industrial data collection that supplied the database for this stage of the research comprised the continuous monitoring period of stockpile 1, beginning on December 12, 2023, at 1:06 p.m. and ending on December 17, 2023, at 1:00 a.m. This operational window yielded a final matrix of 417 valid process records, illustrated in Figure 2, with raw data provided by the mining company's process team and containing balanced samples for both reagents in a real industrial setting.

Figure 2

Excerpt from the integrated raw data matrix

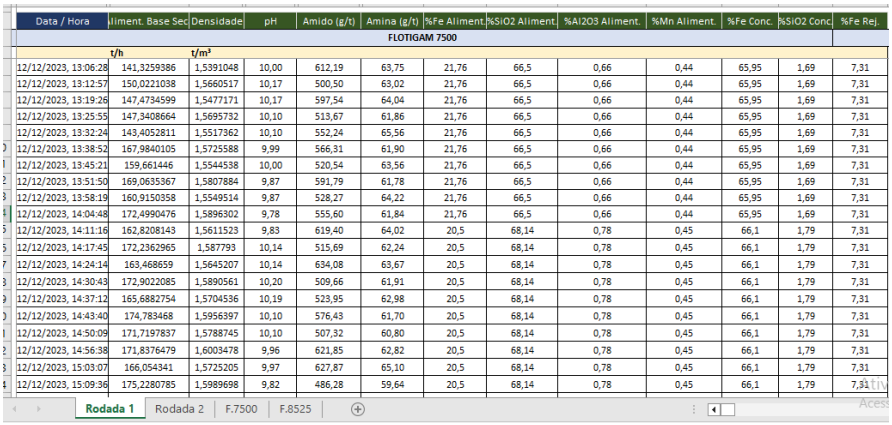

Data / Hora	liment. Base Sec	Densidade	pH	Amido (g/t)	Amina (g/t)	%Fe Aliment.	%SiO2 Aliment.	%Al2O3 Aliment.	%Mn Aliment.	%Fe Conc.	%SiO2 Conc	%Fe Rej.
					FLOTIGAM 7500							
	t/h	t/m³										
12/12/2023, 13:06:28	141,3259386	1,5391048	10,00	612,19	63,75	21,76	66,5	0,66	0,44	65,95	1,69	7,31
12/12/2023, 13:12:57	150,0221038	1,5660517	10,17	500,50	63,02	21,76	66,5	0,66	0,44	65,95	1,69	7,31
12/12/2023, 13:19:26	147,4734599	1,5477171	10,17	597,54	64,04	21,76	66,5	0,66	0,44	65,95	1,69	7,31
12/12/2023, 13:25:55	147,3408664	1,5695732	10,10	513,67	61,86	21,76	66,5	0,66	0,44	65,95	1,69	7,31
12/12/2023, 13:32:24	143,4052811	1,5517362	10,10	552,24	65,56	21,76	66,5	0,66	0,44	65,95	1,69	7,31
12/12/2023, 13:38:52	167,9840105	1,5725588	9,99	566,31	61,90	21,76	66,5	0,66	0,44	65,95	1,69	7,31
12/12/2023, 13:45:21	159,661446	1,5544538	10,00	520,54	63,56	21,76	66,5	0,66	0,44	65,95	1,69	7,31
12/12/2023, 13:51:50	169,0635367	1,5807884	9,87	591,79	61,78	21,76	66,5	0,66	0,44	65,95	1,69	7,31
12/12/2023, 13:58:19	160,9150358	1,5549514	9,87	528,27	64,22	21,76	66,5	0,66	0,44	65,95	1,69	7,31
12/12/2023, 14:04:48	172,4990476	1,5896302	9,78	555,60	61,84	21,76	66,5	0,66	0,44	65,95	1,69	7,31
12/12/2023, 14:11:16	162,8208143	1,5611523	9,83	619,40	64,02	20,5	68,14	0,78	0,45	66,1	1,79	7,31
12/12/2023, 14:17:45	172,2362965	1,587793	10,14	515,69	62,24	20,5	68,14	0,78	0,45	66,1	1,79	7,31
12/12/2023, 14:24:14	163,468659	1,5645207	10,14	634,08	63,67	20,5	68,14	0,78	0,45	66,1	1,79	7,31
12/12/2023, 14:30:43	172,9022085	1,5890561	10,20	509,66	61,91	20,5	68,14	0,78	0,45	66,1	1,79	7,31
12/12/2023, 14:37:12	165,6882754	1,5704536	10,19	523,95	62,98	20,5	68,14	0,78	0,45	66,1	1,79	7,31
12/12/2023, 14:43:40	174,783468	1,5956397	10,10	576,43	61,70	20,5	68,14	0,78	0,45	66,1	1,79	7,31
12/12/2023, 14:50:09	171,7197837	1,5788745	10,10	507,32	60,80	20,5	68,14	0,78	0,45	66,1	1,79	7,31
12/12/2023, 14:56:38	171,8376479	1,6003478	9,96	621,85	62,82	20,5	68,14	0,78	0,45	66,1	1,79	7,31
12/12/2023, 15:03:07	166,054341	1,5725205	9,97	627,87	65,10	20,5	68,14	0,78	0,45	66,1	1,79	7,31
12/12/2023, 15:09:36	175,2280785	1,5989698	9,82	486,28	59,64	20,5	68,14	0,78	0,45	66,1	1,79	7,31

Rodada 1 | Rodada 2 | F.7500 | F.8525

Source: dados cedidos pelo time de processos da mineradora.

The process data describing flotation hydrodynamics and operation were automatically extracted from the Plant Information Management System (PIMS), whose records from field sensors and meters are consolidated and exported in spreadsheet format. Owing to the exception-based storage and data compression guidelines of the supervisory system, the online instrumentation parameters were recorded at an average frequency of one reading every few minutes, ranging from 1 to 7 minutes.

The plant instrumentation system continuously monitored five critical process variables, established as operational predictors: flotation feed rate, measured in tonnes per hour (t/h) and calculated on a dry basis using ore and pulp density; feed pulp density (g/cm³); flotation circuit pH, continuously monitored by an industrial pH meter connected to the supervisory system; specific corn starch dosage (depressant), expressed in grams per tonne of ore (g/t), calculated from online data on diluted starch flow rate and flotation feed rate; and specific collector dosage (FLOTIGAM 7500 or 8525), also expressed in grams per tonne of ore (g/t), calculated from online data on diluted amine flow rate and flotation feed rate.

In parallel with the continuous instrumentation data, the plant's metallurgical and quality-control monitoring is based on laboratory chemical analyses. Unlike electronic sensors, obtaining chemical grades in large-scale plants requires physical time for sampling, preparation, and measurement, making minute-scale acquisition rates impracticable.

At the evaluated unit, the protocol employs hourly composite sampling. Manual cutters collect physical pulp increments every 15 minutes directly from the pipeline streams. At the end of each hour, these four increments are combined, generating a composite sample representative of that hour of operation. This sample is sent to the plant's physicochemical laboratory, where it undergoes sequential filtration, oven drying, mechanical pulverization, and homogenization steps for the preparation of pressed pellets. Finally, quantitative grade determination is performed by X-ray Fluorescence Spectrometry (XRF).

The chemical parameters routinely analyzed and collected for this research included: in the flotation feed, the percentage grades of iron, silica, alumina, and manganese; in the flotation concentrate, the percentage grades of silica and iron; and in the flotation tailings, the percentage grade of iron.

To ensure the physical consistency and mathematical robustness of the predictive models, temporal alignment was applied to the database extracted from PIMS. Since the industrial flotation process does not occur instantaneously, the variables were synchronized with the response variables from the chemical analyses using a fixed delay calculated based on the average nominal hydraulic residence time of the flotation columns, as determined by the flotation process team. This preprocessing step was essential to mitigate mass-lag noise, ensuring that the Artificial Neural Network properly correlated the characteristics of the same ore parcel throughout the operating circuit.

To enable modeling using the Artificial Neural Network, it became essential to unify the discrete laboratory data, recorded hourly, with the semicontinuous field instrumentation data, recorded every few minutes, into a single coherent training matrix.

Because industrial flotation operates under continuous-flow conditions and large volumes, which provide high physicochemical inertia to the tanks, and because the hourly XRF analysis is a true composite average of four increments distributed throughout that hour, the hourly-window replication method was adopted. Mathematically, the chemical grade value determined for each hour was repeated and inserted into all online instrumentation rows whose sampling was performed within the corresponding date-and-hour period. This approach preserved the representativeness and physical causality of the process, allowing

each row of the final spreadsheet to reflect an instantaneous plant state in which chemical conditions, represented by laboratory grades, and operational variables, represented by sensors, acted simultaneously on the circuit.

The selection of the data to be analyzed was based on the variables routinely collected by the flotation circuit, encompassing both flotation process data and chemical analysis data.

The methodological decision to structure a rigorous database auditing and cleaning stage, using Data Clean routines in MATLAB software, derives directly from the main technological barriers identified in the international mineral-processing literature. Previous industrial studies have reported that the systematic occurrence of instrumentation noise, failures in industrial sensor readings, and physical sampling delays generate severe anomalies that destabilize the training process and prevent the adaptive convergence of neural networks (Costa *et al*., 2022; Bendaouia *et al*., 2024). Therefore, the filtering methods and signal reconstruction performed in this section directly mitigate these inconsistencies, ensuring the statistical reliability required for subsequent modeling.

After consolidation and temporal alignment of the instrumentation and laboratory chemical analysis matrices, the raw database was imported into the MATLAB computational environment to perform the integrity auditing stage. The initial anomaly screening was carried out using MATLAB's interactive Data Clean tool. Through descriptive statistical analysis and visual inspection of scatter plots and box plots, the behavior of all variables comprising the study was evaluated.

The diagnosis revealed that the process variables, such as pH, pulp density, feed rate, and all chemical grades determined by X-ray fluorescence, fell within statistically acceptable ranges, operating within metallurgically acceptable limits and without evidence of spurious readings or signal failures.

The only class of anomalies identified was concentrated exclusively in the specific reagent dosage variables, namely starch and etheramine, expressed in g/t. The Data Clean application detected the presence of isolated discrepant points, or outliers, characterized by abrupt and instantaneous drops in dosage values to zero, followed by an immediate return to the nominal operating level in the subsequent record. Figure 3 shows the data processed using MATLAB's Data Clean tool, with the data shown in blue and the discrepant points in red. The first plot refers to starch dosage, the depressant, and the second to etheramine, the collector.

Figure 3

Time-series scatter plot of reagent dosage

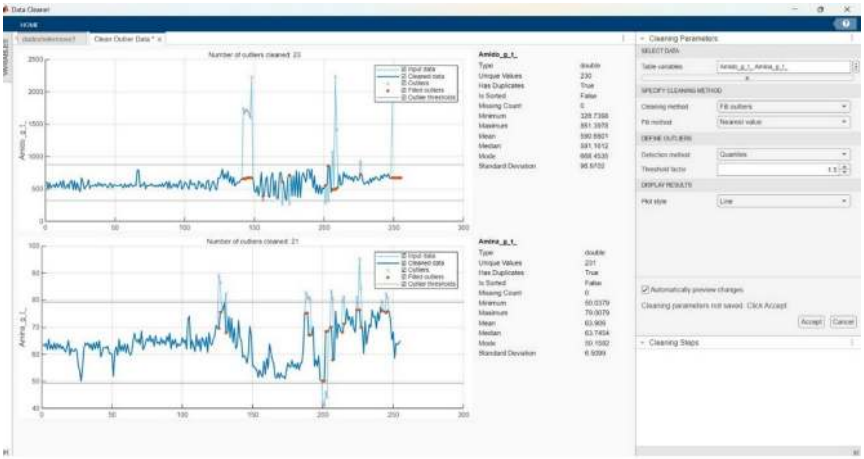

Source: The Authors.

In a technical analysis conducted with the flotation operations team, it was found that these discrepant readings did not reflect an actual physical failure in reagent supply. At the evaluated plant, the dosage variables expressed in grams per tonne do not originate from a direct sensor reading, but rather from an internal calculation layer within the supervisory system, which processes the volumetric reagent flow rate by cross-referencing it with the dry ore feed rate and pulp density. Millisecond-scale momentary failures in the electrical transmission signal of any of these three meters induced the computational calculation to momentarily zero or spike the record in the PIMS, even though the physical closed-loop control system continued to consistently deliver the required dosage through the dosing pumps.

Based on this operational evidence, complete deletion of the rows containing these dosage outliers was ruled out. Since all other variables in the same row, including feed rate, density, and pH, were perfectly consistent and stable, deleting the record would represent an unnecessary loss of data and would weaken the network training. Therefore, vector preservation of the row was adopted through adaptive replacement treatment.

To correct the dosage data failures without distorting process variability, the discrepant points were treated directly in MATLAB using a local quadratic interpolation and normalization routine based on the nearest neighboring values. The tool replaced the spurious null value by fitting a polynomial function calculated over the time window immediately before and after the failure event. This procedure smoothly filled the numerical gaps, mirroring the actual stability

occurring at industrial scale and ensuring a continuous and mathematically consistent data matrix.

The flotation circuit modeling was structured using a Multilayer Perceptron (MLP) Artificial Neural Network architecture, implemented with the MATLAB Deep Learning Toolbox. The mathematical objective of the network is to learn the functional mapping that connects the multidimensional space of the plant's operational variables with the metallurgical quality indicators obtained in the laboratory.

The definition of the data vectors strictly followed the fundamental control parameters described in the industrial routine. Thus, the model input layer was configured with 10 predictor neurons, divided among physical feed characteristics, physicochemical control variables, and feed mineral grades. In turn, the output layer was designed with 3 target neurons, predicting iron grade (%Fe) in the concentrate, silica grade (%SiO_2) in the concentrate, and iron grade (%Fe) in the tailings. The distribution of variables in the network topology followed the structure consolidated in Table 1.

Table 1

Vector configuration of the ANN input and output layers

Network Layer	Variable Type	Operational Parameter	Unit	Data Nature
Input	Operational	Plant Feed Rate	t/h	Online Instrumentation
	Operational	Feed Pulp Density	g/cm³	Online Instrumentation
	Operational	Flotation Circuit pH	Dimensionless	Online Instrumentation
	Chemical / Control	Specific Depressant Dosage (Starch)	g/t	PIMS
	Chemical / Control	Specific Collector Dosage (Amine)	g/t	PIMS
	Mineralogical	Iron Grade (%Fe) in the Feed	%	Laboratory XRF
	Mineralogical	Silica Grade (%SiO_2) in the Feed	%	Laboratory XRF
	Mineralogical	Alumina Grade (%Al_2O_3) in the Feed	%	Laboratory XRF
	Mineralogical	Manganese Grade (%Mn) in the Feed	%	Laboratory XRF
Output	Metallurgical	Iron Grade (%Fe) in the Concentrate	%	Laboratory XRF
	Metallurgical	Silica Grade (%SiO_2) in the Concentrate	%	Laboratory XRF

	Metallurgical	Iron Grade (%Fe) in the Tailings	%	Laboratory XRF

Source: Prepared by the authors.

To comparatively evaluate the technological replacement without the noise of plant variations, two independent neural network structures were developed within the sampling environment of stockpile 1: one network trained exclusively with the data matrix corresponding to the standard collector FLOTIGAM 7500 and another trained with the data from the FLOTIGAM 8525 collector. As cross-validation of the environment, the behavior of the networks was tested by applying the maximum and minimum data limits of one product to the architecture of the other, yielding highly stable and similar responses. This procedure mathematically demonstrated that the industrial experiment was conducted under analogous plant operational and geological conditions, validating the robustness of the direct comparison between the reagents.

For the internal structuring of the models, MATLAB's cross-validation protocol was applied, in which the campaign data rows were randomly and independently partitioned by the software, following fixed proportions of 70% for training, 15% for validation, and 15% for independent testing with unseen data.

The algorithm selected for optimizing the synaptic weights and biases was Levenberg-Marquardt (LM). The Early Stopping mechanism was activated to monitor the Mean Squared Error (MSE) of the validation set, interrupting the iterative process when the validation error increased for consecutive cycles, thereby safeguarding the network against overfitting.

The activation function used in the hidden layer was the hyperbolic tangent function (tansig), while the output layer used the linear function (purelin).

A neural-network simulation was performed under variation of iron (20% to 25%), manganese (0.34% to 0.44%), and aluminum (0.66% to 0.82%) grades in the feed. To isolate the effect of these variables, the remaining operational parameters were kept static at their historical process average values, as shown in Table 2.

Table 2

Summary of input statistical data

Data Summary

DataType	table
NumVariables	12
NumObservations	163
NumVarsWithMissing	0
NumVarsWithDuplicates	11

		6 Minimum	7 Maxim...	8 Mean	9 Median	10 Mode	11 Standard Deviation
1	Aliment_BaseSeca	117.6597	233.6691	171.2741	176.8471	117.6597	26.6329
2	Densidade	1.4480	1.6044	1.5387	1.5398	1.5131	0.0305
3	pH	9.0498	10.3695	10.0411	10.0484	9.7908	0.2154
4	Amido_g_t_	201.0158	740.9405	482.3307	469.7045	600	98.8682
5	Amina_g_t_	30.7192	74.0006	51.5411	50	60	8.1403
6	x_FeAliment_	21.7400	24.8800	23.3623	23.3000	23.4400	0.9086
7	x_SiO2Aliment_	62.0700	66.3500	64.4699	64.4500	64.4300	1.2968
8	x_Al2O3Aliment_	0.5000	0.9800	0.6858	0.6400	0.5000	0.1341
9	x_MnAliment_	0.2500	0.4200	0.3100	0.3000	0.2900	0.0376
10	x_FeConc_	66.3700	67.2900	66.6860	66.6300	66.6300	0.2462
11	x_SiO2Conc_	0.8700	1.5800	1.0912	1.0300	1.0300	0.2246
12	x_FeRej_	8.3100	14.8900	9.9067	9.5100	10.2600	1.6943

Source: Prepared by the authors.

4 RESULTS

Figure 4 shows that the neural network training converged after 49 epochs, with the best validation performance; the final mean squared error reached 9.1 × 10−21.

Figure 4

Neural network evaluation: training, validation, and testing

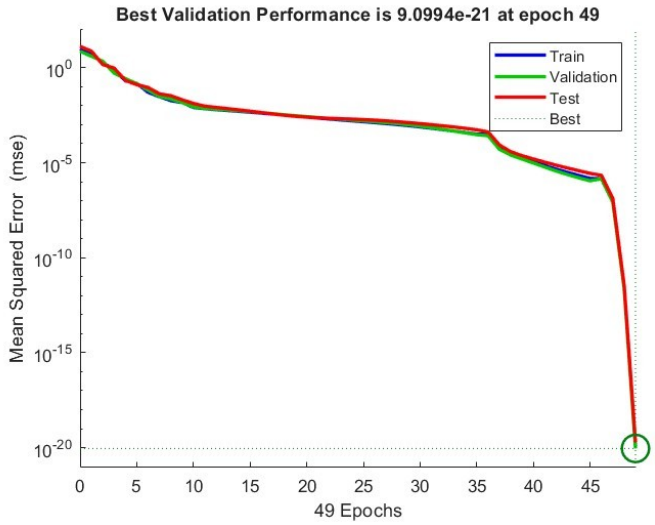

Source: The Authors.

Given the high coefficient of determination (R2) values obtained during the model testing phase, as illustrated in Figure 9, and in order to rule out potential overfitting effects, a rigorous empirical validation of physical consistency was performed. To this end, the neural network was extensively tested through queries using real and known operational data

vectors from the plant, based on historical records independent of those used for training. The responses generated by the computational model demonstrated strict coherence and convergence with the actual metallurgical results observed at the plant, statistically validating the profile and slope of the parametric sweep curves subsequently generated.

Figure 5

Correlation coefficients for training, validation, testing, and overall performance

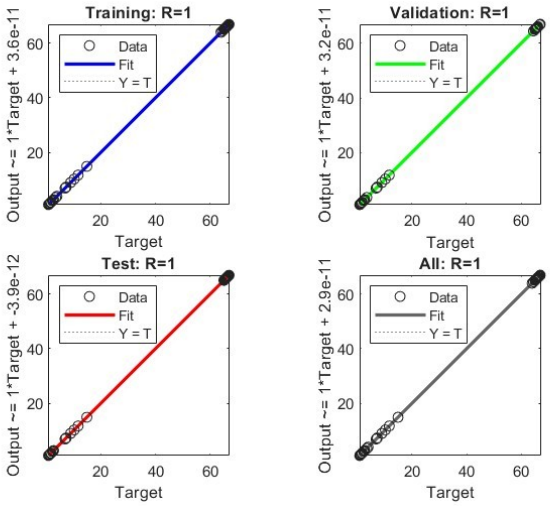

Source: The Authors.

Figure 5 shows the fit of the predictive neural-network model, demonstrating a linear correlation coefficient (R) above 0.85, with R values reaching close to 1.

The process of defining the optimal number of neurons in the hidden layer was conducted iteratively using an empirical trial-and-error method, evaluating architectures ranging from 1 to 50 neurons. The topology that presented the best performance and stability profile consisted of 10 neurons in the hidden layer and 3 target neurons, as illustrated in Figure 6.

Figure 6

Schematic illustration of the neural network

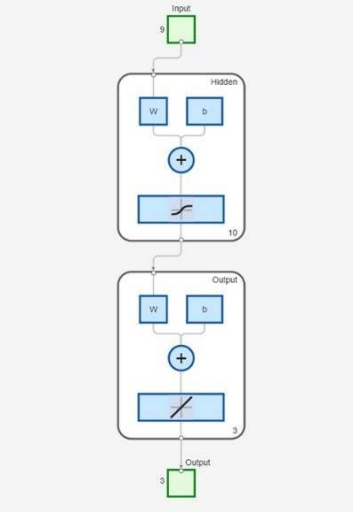

Source: The Authors.

Figure 7 presents the results of the final neural-network simulation, performed under variation of iron (20% to 25%), manganese (0.34% to 0.44%), and aluminum (0.66% to 0.82%) grades in the feed.

To isolate the effect of these variables, the remaining operational parameters were kept static at their historical process average values, as detailed in Table 2 of the methodology.

Figure 7

Predictive neural-network simulation – Percentage iron grade in the concentrate

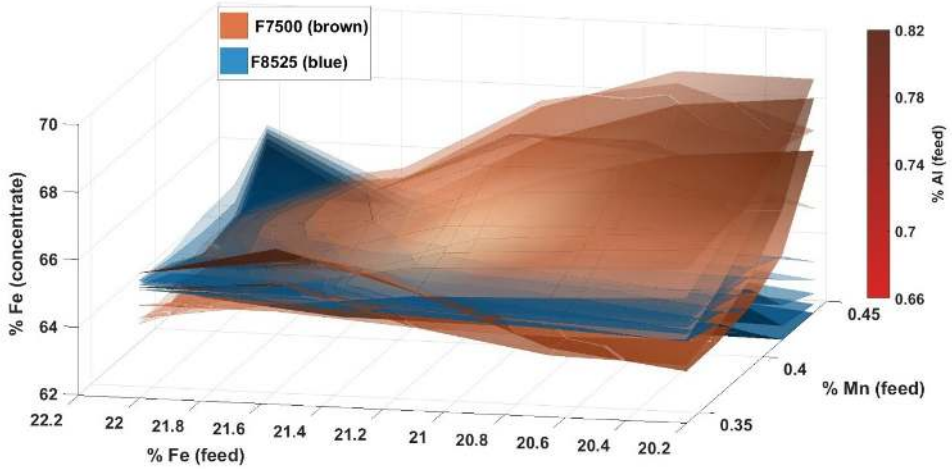

Source: The Authors.

Analysis of Figure 7, based on the predictive neural-network simulation, shows that FLOTIGAM 7500 produced higher percentages of iron in the concentrate than FLOTIGAM

8525 within the specific range of the database analyzed.

Figures 8 and 9 show the results for iron grade in the tailings obtained using predictive neural-network simulation for the specific range of the database analyzed.

Figure 8

Predictive neural-network simulation – Iron grade in the tailings

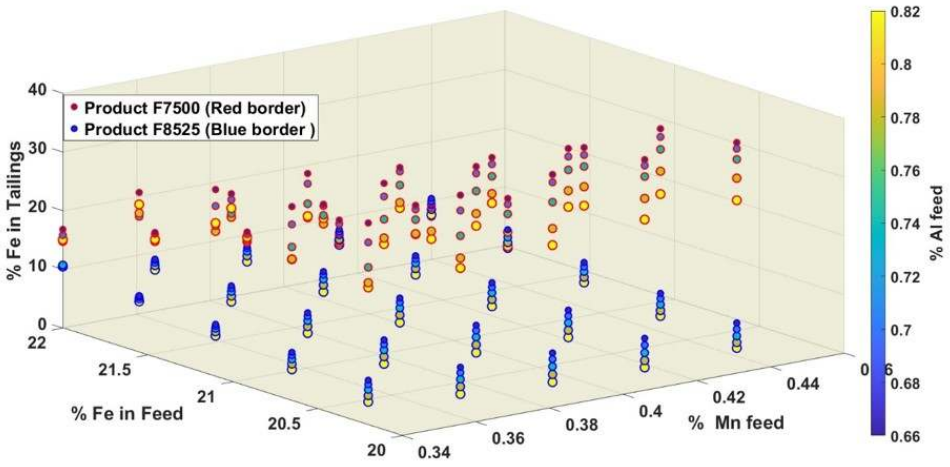

Source: The Authors.

Figure 9

Color map – Predictive neural-network simulation – Iron grade in the tailings

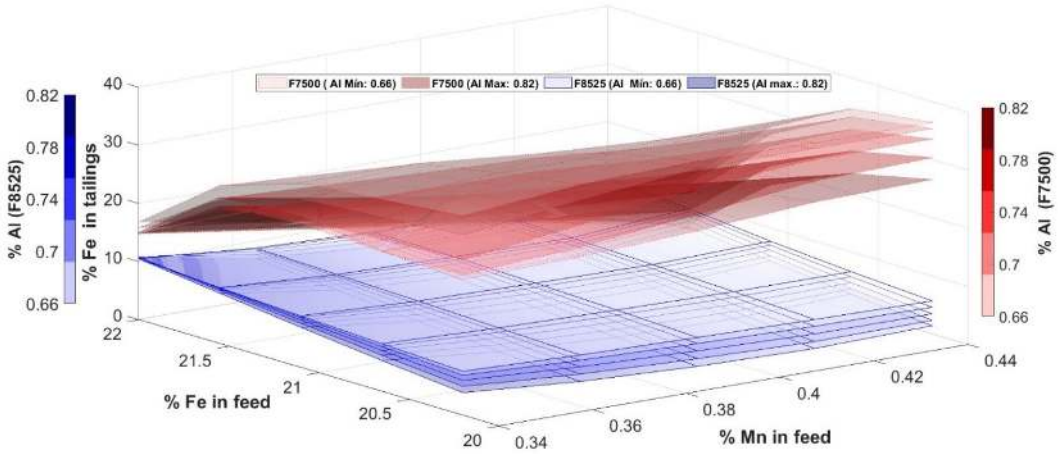

Source: The Authors.

Figures 8 and 9 reveal that FLOTIGAM 8525 generated lower percentages of iron in the tailings than FLOTIGAM 7500. Regarding the percentage of Fe in the tailings, FLOTIGAM 8525 performed better than FLOTIGAM 7500.

The analysis of Figures 7, 8, and 9 reveals competitive behavior between the reagents: while the FLOTIGAM 7500 collector shows greater efficiency in terms of iron grade in the concentrate, FLOTIGAM 8525 stands out for the lower iron grade obtained in the tailings. This complementarity enables process optimization through artificial neural networks by simulating the variability of iron, aluminum, and manganese grades in the feed to project the response profiles of iron grade in both the concentrate and the tailings, thereby determining the respective maximum points (maximization of product grade) and minimum points (minimization of losses). Figure 10 shows the process optimization analysis.

Figure 10

Process optimization analysis

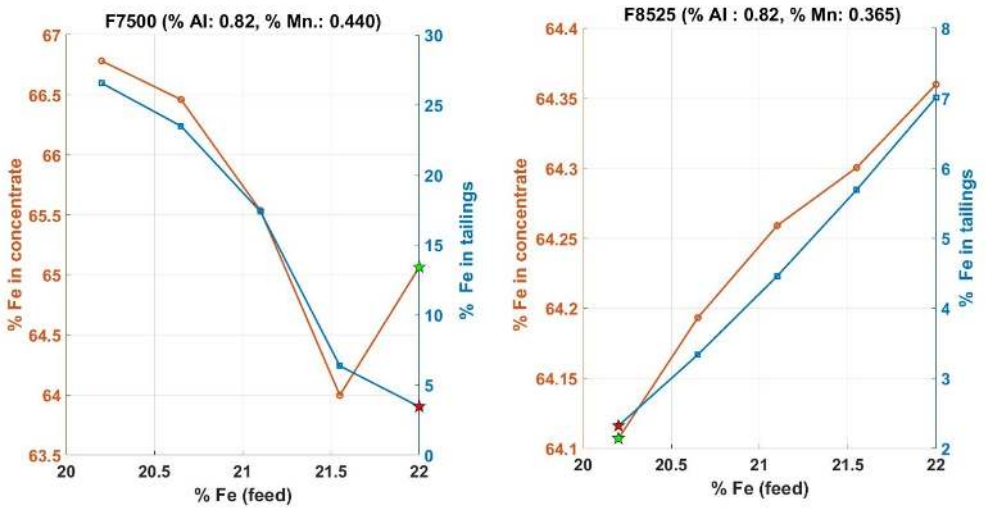

Source: The Authors.

Based on the profiles generated by the neural-network simulation, it is concluded that the optimal process points vary significantly between the reagents due to each reagent's sensitivity to the iron grade in the feed.

For the FLOTIGAM 7500 collector, the most strategic operating point is found at 22% Fe in the feed, where the system reaches its minimum tailings-loss point (3%, red star), substantially reducing the iron losses observed at lower feed grades while still ensuring an excellent-quality concentrate with approximately 65.1% Fe (green star).

FLOTIGAM 8525 exhibits a much more stable and controlled upward linear behavior across the entire range. It reaches the absolute minimum iron grade in the tailings (~2.1%, green star) with a feed grade of 20.2% Fe, although operating this circuit at 22% Fe in the feed may be preferable because it maximizes the concentrate grade to its highest level (~64.36%)

while maintaining tailings losses at a tolerable level of 7%. Thus, the neural networks reveal that, while FLOTIGAM 7500 requires strict operational control fixed at 22% feed grade to contain iron losses, FLOTIGAM 8525 offers greater robustness and flexibility, allowing the operator to alternate between maximum product purity (at 22% feed grade) and maximum metallurgical recovery (at 20.2% feed grade).

5 CONCLUSION

Computational modeling using Artificial Neural Networks, followed by parametric sensitivity analyses, made it possible to accurately map the operational signatures of the FLOTIGAM 7500 and FLOTIGAM 8525 collectors under the geometallurgical variability of the plant feed.

The analysis revealed competitive behavior between the reagents: while the FLOTIGAM 7500 collector showed greater efficiency in terms of iron grade in the concentrate, FLOTIGAM 8525 stood out for the lower iron grade obtained in the tailings. This complementarity enabled process optimization through artificial neural networks by simulating the variability of iron, aluminum, and manganese grades in the feed to project the response profiles of iron grade in the concentrate and in the tailings, thereby determining the respective maximum points (maximization of product grade) and minimum points (minimization of losses).

The neural network proved to be an effective tool for studies of multivariable industrial operations under transient conditions, such as reverse cationic flotation of iron ore.

REFERENCES

ALI, D.; FRIMPONG, S. Mining 4.0: concept, technologies and applications. **Journal of Mining and Environment**, [s. l.], 2020.

ARAÚJO, A. C.; VIANA, P. R. M.; PERES, A. E. C. Reagents in iron ores flotation. **Minerals Engineering**, [s. l.], v. 18, p. 219-224, 2005.

BENDAOUIA, A. *et al.* Artificial intelligence for enhanced flotation monitoring in the mining industry: a ConvLSTM-based approach. **Computers & Chemical Engineering**, [s. l.], v. 180, p. 108476, 2024.

CHAVES, A. P. **Teoria e Prática do Tratamento de Minérios: A Flotação no Brasil.** 3. ed. São Paulo: Oficina de Textos, 2009. v. 4.

CHAVES, A. P. **Teoria e Prática do Tratamento de Minérios: Bombeamento de polpas e classificação**. v. 1. 3. ed. São Paulo: Oficina de Textos, 2006.

COSTA, A. C. A. A. *et al*. Deep **architecture for silica forecasting of a real industrial froth flotation process. Engineering Applications of Artificial Intelligence**, [s. l.], v. 115, p. 105196, 2022.

FILIPPOV, L. O.; SEVEROV, V. V.; FILIPPOVA, I. V. An overview of the beneficiation of iron ores via reverse cationic flotation. **International Journal of Mineral Processing**, [s. l.], v. 127, p. 62-69, 2014.

JORJANI, E. *et al*. Application of artificial neural networks in mineral processing: a review. **Physicochemical Problems of Mineral Processing**, [s. l.], v. 43, p. 221-240, 2009.

LIMA, N. P.; VALADÃO, G. E. S.; PERES, A. E. C. Effect of amine and starch dosages on the reverse cationic flotation of an iron ore. **Minerals Engineering**, [s. l.], 2013.

LIMA, R. M. F.; QUIRINO, L. Efeito da adsorção de amina no potencial zeta da hematita e do quartzo. **Rem: Revista Escola de Minas**, Ouro Preto, v. 56, n. 3, p. 203-207, 2003.

NAPIER-MUNN, T. Statistical Methods for Mineral Engineers: How to Design Experiments and Analyse Data. **Brisbane: Julius Kruttschnitt Mineral Research Centre (JKMRC),** 2014.

PAPINI, R. M.; COELHO, J. M.; PERES, A. E. C. Influence of froth stability on the performance of iron ore flotation. **Minerals & Metallurgical Processing**, [s. l.], 2001.

PERES, A. E. C. *et al*. Reagents in iron ore flotation**. REM - Revista Escola de Minas**, [s. l.], 2007.

POUYANFAR, S. *et al*. A survey on deep learning: algorithms, techniques, and applications. **ACM Computing Surveys**, [s. l.], v. 51, n. 5, p. 1-36, 2018.

ROCHA, L.; CANÇADO, R. Z. L.; PERES, A. E. C. Iron ore flotation in the presence of alumina. **Minerals Engineering**, [s. l.], v. 23, n. 11-13, p. 842-845, 2010.

VALADÃO, G. E. S.; ARAÚJO, A. C. **Introdução ao Tratamento de Minérios**. Belo Horizonte: Editora UFMG, 2012.

WANG, L. *et al*. Flotation of quartz from iron ore using a novel low-foaming cationic collector. **Chemical Engineering Research and Design**, [s. l.], 2015.